ISSN 1029-9599, Physical Mesomechanics, 2014, Vol. 17, No. 4, pp. 265–273. © Pleiades Publishing, Ltd., 2014.
Original Text © R. Wetter, V.L. Popov, 2014, published in Fizicheskaya Mezomekhanika, 2014, Vol. 17, No. 3, pp. 31–38.

Influence of the Alignment of Load and Oscillation on the Frictional Shakedown of an Elastic Rolling Contact with Coulomb Friction

R. Wetter[1]* and V. L. Popov[1, 2, 3]

[1] *Technische Universität Berlin, Berlin, 10623 Germany*
[2] *National Research Tomsk State University, Tomsk, 634050 Russia*
[3] *National Research Tomsk Polytechnic University, Tomsk, 634050 Russia*
** e-mail: r.wetter@tu-berlin.de*

Received February 17, 2014

Abstract—We examine frictional shakedown of a three dimensional elastic rolling contact. Slight oscillatory rolling of one contacting body varies the normal pressure distribution. In turn this causes incremental sliding processes and a macroscopic rigid body motion. We consider two settings: tangential force and rolling direction aligned parallel and perpendicular to each other. In both cases, the slip ceases after the first few periods and a safe shakedown occurs if the oscillation is sufficiently small. Otherwise ratcheting occurs and the accumulated slip leads to a continuing rigid body motion.

Numerical simulations with Kalker's and Vollebregt's software CONTACT show that the rolling direction leads to differences in the contact region and the traction distribution. Using the method of dimensionality reduction we derive the analytical shakedown limits for the tangential load and the oscillation amplitude. The results show strong agreement with experimental data and allow the accurate prediction of the shakedown displacement and the maximum tangential load capacity in the shakedown state. It shows that a perpendicular alignment of force and rolling direction increases the final displacement in case of shakedown as well as the incremental shift in case of ratcheting.

DOI: 10.1134/S1029959914040031

Keywords: elastic rolling contact, Coulomb friction, vibrations, frictional shakedown, ratcheting, method of dimensionality reduction

1. INTRODUCTION

Force locked connections are used in various technical applications, e.g. bolted connections, interference fits and machining fixtures. The tangential load capacity $F_{t,max}$ of these systems is mainly controlled by the tangential contact properties [1–5]. According to Coulomb's law $F_{t,max}$ is determined by the macroscopic normal force F_n and the friction coefficient μ:

$$F_{t,max} = \mu F_n. \quad (1)$$

If this force is exceeded, complete sliding occurs and the contact fails. However, in many technical systems the frictional contact is also affected by vibrations. For instance, the macroscopic forces can consist of a static part superposed with small oscillations. Or the point of application of the forces somehow shifts, what leads to oscillations of the pressure and traction distributions [6]. Both scenarios cause a periodic incremental slip of the contact interface, even if the tangential force is far below the maximum load of Eq. (1), i.e. appears insufficient to initiate complete sliding. This effect is responsible for microslip [7] and fretting fatigue [8, 9] of the relevant components. In some cases, the initial slip ceases after the first few periods due to a residual force in the interface, sufficiently strong to prevent any further slip [10, 11]. Consequently, the entire contact will finally remain in a state of stick, even if the oscillation is continued. This process is referred to as frictional shakedown, due to the analogy to plasticity problems, where shakedown describes a process in which the deformed bodies only show plastic strain in the first few loading cycles and pure elastic response in the steady state. Consequently, the Melan theorem for plastic shakedown [12] was transferred to discrete [13] and continuous systems [14] with Coulomb friction and complete contact, meaning that the contact area does not change during the oscillation.

In the authors recent works [15, 16] the oscillating elastic rolling contact was introduced as an example for an incomplete or advancing contact, in which the contact area changes during oscillation. The exact analytical shakedown limits were formulated and it was shown, that shakedown is accompanied with a significant decrease of the maximum tangential load capacity. In the latter study [16] the oscillation was aligned parallel to the tangential loading. In the current study, we examine the case that the oscillation and the loading are perpendicular to each other. Again, we use numerical and experimental analysis to give the exact shakedown limits and determine the influence on the load capacity.

2. MODELS AND METHODS

Firstly, we consider a tangentially loaded Hertzian contact of a rigid sphere and an elastic flat substrate. The system is assumed to be uncoupled, meaning that variations in normal forces will not induce any tangential displacement and vice versa. This requires Dundurs' constant $\beta = 0$ as it is the case for frictionless contacts, similar materials, incompressible materials or if one body is rigid and the other one is incompressible [17]. A good description for the initial static tangential contact can be found, for example in Popov [18]. An alternative approach refers to Ciavarella [19] and Jäger [20], where the tangential contact quantities are determined on the basis of the normal problem and a correctional term. However, the elastic properties of the substrate E^* and G^* as well as its radius R are chosen as effective quantities of a contact of two elastic spheres with particular radii R_i, shear moduli G_i and Poisson ratios ν_i:

$$E^* = \left(\frac{1-\nu_1}{G_1} + \frac{1-\nu_2}{G_2} \right)^{-1}, \quad G^* = \left(\frac{2-\nu_1}{4G_1} + \frac{2-\nu_2}{4G_2} \right)^{-1}, \quad R = \left(\frac{1}{R_1} + \frac{1}{R_2} \right)^{-1}. \tag{2}$$

The normal force F_n leads to the indentation depth d, which is defined as the vertical displacement of the rigid sphere

$$d = \left(\frac{3}{4} \frac{F_\mathrm{n}}{E^* R^2} \right)^{2/3}. \tag{3}$$

The area of contact is delimited by the contact radius $a = \sqrt{Rd}$. Assuming Coulomb friction with coefficient μ, a tangential loading F_t, insufficient to cause complete sliding, will lead to a slight rigid body displacement of the substrate [18]

$$U_\mathrm{stat} = \mu \frac{E^*}{G^*} d \left(1 - \left(1 - \frac{F_\mathrm{t}}{\mu F_\mathrm{n}} \right)^{2/3} \right) \tag{4}$$

in the same direction. Initially, slipping will only occur at the boundary region of the contact area, whereas the center region remains in a state of stick and is delimited by the stick radius [18]

$$c = a \left(1 - \frac{F_\mathrm{t}}{\mu F_\mathrm{n}} \right)^{1/3}. \tag{5}$$

In the next step, this static tangential contact is superposed by a slight oscillatory rolling of the sphere with amplitude W, being the lateral movement of the sphere center, as depicted in Fig. 1.

The system is assumed to be quasi-static, meaning that we assume a constant μ and neglect inertia effects. This is valid as long as the rolling is slower than the propagation speed of elastic waves within the body. In addition to the parallel case $(W \parallel F_\mathrm{t})$ as considered in [16], we consider a perpendicular setting $(W \perp F_\mathrm{t})$ as depicted in Fig. 1. Again, the overall macroscopic load will be kept constant. Thus, the rolling does not lead to any additional friction force or momentum but changes the pressure distribution and the actual contact area. According to this, the problem setting is equivalent to a frictional contact with constant macroscopic forces, which is exposed to a rocking of the contacting bodies, i.e. varying point of application of the normal force [6].

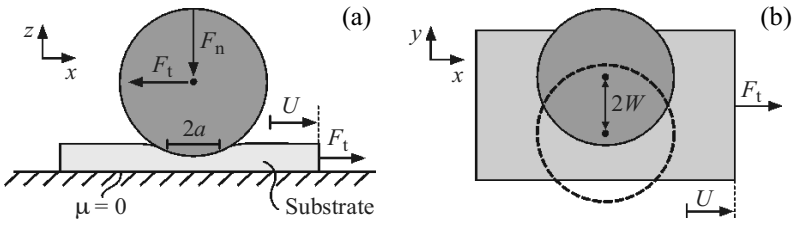

Fig. 1. Static tangential contact of a rigid sphere and an elastic substrate (a); oscillating, elastic rolling contact with lateral movement of the center W, perpendicular to the tangential force (b).

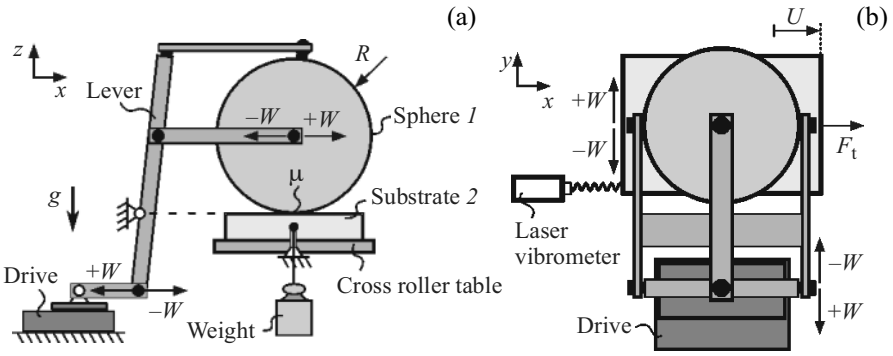

Fig. 2. Experimental setting: steel sphere (*1*), silicone rubber substrate (*2*), weight, drive PI-M 405-DG and laser-vibrometer Polytec OFV-5000.

2.1. Experimental Setting

The test rig for $W \perp F_t$ is depicted in Fig. 2. It consists of a sphere *1* made of ST-52 steel and a silicon-rubber substrate *2*. Thus, the system is almost uncoupled as $\beta = 0$. All important parameters are listed in Table 1. In order to minimize external influences, the substrate is put on a low friction cross roller table. Its resistance force of $F_r = 0.1$ N lowers the actual tangential force, which itself is controlled by a single weight m_W that is connected to the substrate through a string. Hence, the tangential force results to $F_t = F_W - F_r$. The weight of the sphere acts as the normal force $F_n = m_1 g$ and the rolling motion of the sphere is generated by a lever arm construction. Its main bearing is located exactly on the same level as the contact point between sphere and substrate. As this point corresponds to the instantaneous center of motion, the oscillations of the lever-arm result in a pure rolling of the sphere and additional influences on the macroscopic load regime are minimized. To resists the effective moment of the tangential force about the *z*-axis, a massive stiffening plate is used. The back and forth motion of the lever arm is generated by a high-precision linear drive. Finally, the rigid body displacement of the substrate *U* is measured using a high resolution laser vibrometer.

Table 1. Properties of the experimental setting for $W \perp F_t$

R	40 mm
μ	0.93
E_1/E_2	$206 \cdot 10^3/4.35$ MPa
ν_1/ν_2	0.3/0.5
F_n	21.19 N
a	4.8 mm
d	0.57 mm

The first natural frequencies were calculated as 22 Hz for $W \parallel F_t$ and 19 Hz for $W \perp F_t$. This difference is due to the fact that the bending stiffness of the lever arms is lower than their tensile stiffness. Hence in both cases, the lowest natural frequency is two orders higher than the highest excitation frequency, which results to 0.21 Hz for a drive's speed of $\dot{W} = 1$ mm/s. Therefore, the dynamic influences of the test rig can be neglected.

2.2. Three Dimensional Simulation

The well-known CONTACT software package, based on the Kalker theory of rolling contacts [21] is used to conduct a three dimensional quasi-static simulation of the problem. The program uses constant element discretization and nested iteration processes to solve the transient problem of rolling [22]. In our case, a world fixed coordinate system is applied and the geometry is entered using a so-called non-Hertzian approach. Here, the initial distance between the undeformed surfaces of the two bodies is specified through a quadratic function:

$$h(x, y) = \frac{x^2}{2R} + \frac{y^2}{2R}. \quad (6)$$

The rolling is simulated as a stepwise incremental shift of the profile with ΔW being the step size. Thus for $W \perp F_t$ the actual profile after n rolling steps reads:

$$h(x, y) = \frac{1}{2R}x^2 + \frac{1}{2R}y^2 - \frac{n\Delta W}{R}y + \frac{(n\Delta W)^2}{2R}. \quad (7)$$

For a mutual verification, we use the exact parameters of the experimental setup as described in Section 2.1. The number of elements varies with the amplitude, due to the world fixed approach. With a side length of Δx, $\Delta y = 0.2$ mm and an incremental step length of $\Delta W = 0.2$ mm, result 3050–4200 discretization elements. We computed 10 periods of rolling for each combination of tangential loading and amplitude, resulting in

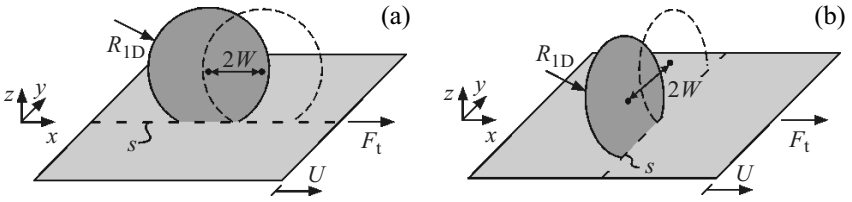

Fig. 3. Equivalent one-dimensional model of the method of dimensionality reduction. System is aligned in the *x*-direction for the parallel case (a) and in the *y*-direction for the perpendicular case (b).

241–681 computation steps or $2h$–$4h$ for each single parameter combination.

2.3. One Dimensional Model Using the Method of Dimensionality Reduction

The method of dimensionality reduction enables an exact mapping of uncoupled, rotationally symmetric tangential contacts with Coulomb friction without loss of essential properties [23, 24]. Using the method of dimensionality reduction, the initial three dimensional system can be modeled by an equivalent one-dimensional elastic foundation of independent springs, as described in [24, 25]. Both, the radius of the foundation $R_{1D} = 1/2\,R$ and its normal and tangential spring stiffness $k_z = E^*\Delta s$ and $k_x = G^*\Delta s$ must be chosen according to the rules of Popov [26] with Δs being the distance between adjacent springs. The model of the method of dimensionality reduction enables a fast and precise simulation of the oscillatory rolling as described in [15]. In addition, the new equilibrium state can be described analytically, from which the shakedown limits can be deduced [16]. The oscillatory rolling is considered using a quasi-static incremental approach. Here, an incremental rolling ΔW changes the normal deflection u_z of a spring at position s:

$$u_z = d - (s \pm \Delta W)^2 / R. \qquad (8)$$

In dependence on the initial model, the coordinate s corresponds either to the x-direction in case that $W \parallel F_t$ or the y-direction in case that $W \perp F_t$, as depicted in Fig. 3. As the method of dimensionality reduction assumes rotational symmetry of the contact region and uncoupled systems [24], the resultant displacements and contact regions for the models of the method of dimensionality reduction of both cases match exactly. According to this, in terms of the method of dimensionality reduction, all findings of the parallel case [16] correspond exactly to the perpendicular case.

3. EXPERIMENTS AND ANALYSIS

The tangential force F_t, the displacement U and the oscillation amplitude W are normalized with the maximum holding force, the maximum tangential displacement [24] and the contact radius:

$$f_t = \frac{F_t}{\mu F_n},\ u = \frac{U}{U_0} = \frac{U}{\mu}\frac{E^*}{G^*}d,\ w = \frac{W}{a}. \qquad (9)$$

We restrict ourselves to tangential forces below the maximum holding force, and oscillation amplitudes smaller than the contact radius:

$$f_t \le 1,\ w \le 1. \qquad (10)$$

Consequently, without oscillatory rolling, no complete sliding will occur and the center of the sphere will

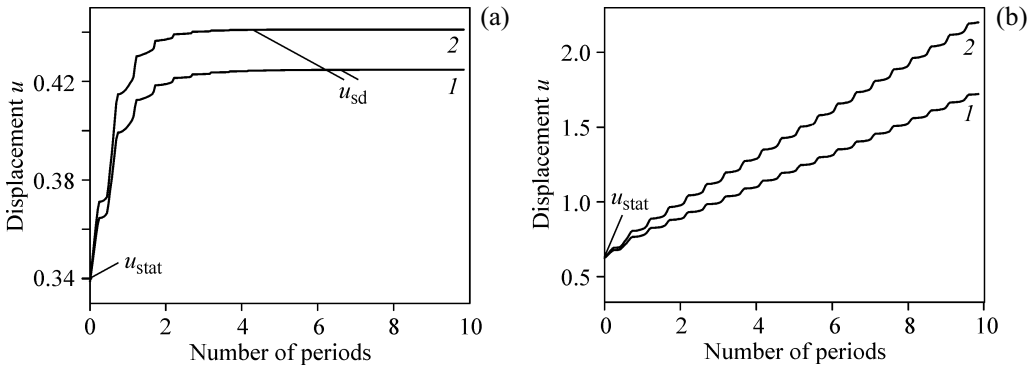

Fig. 4. Displacement of the substrate u for $w \parallel f_t$ (*1*) and $w \perp f_t$ (*2*) with $w = 0.23$. Shakedown for $f_t = 0.46$ (a) and ratcheting for $f_t = 0.77$ (b).

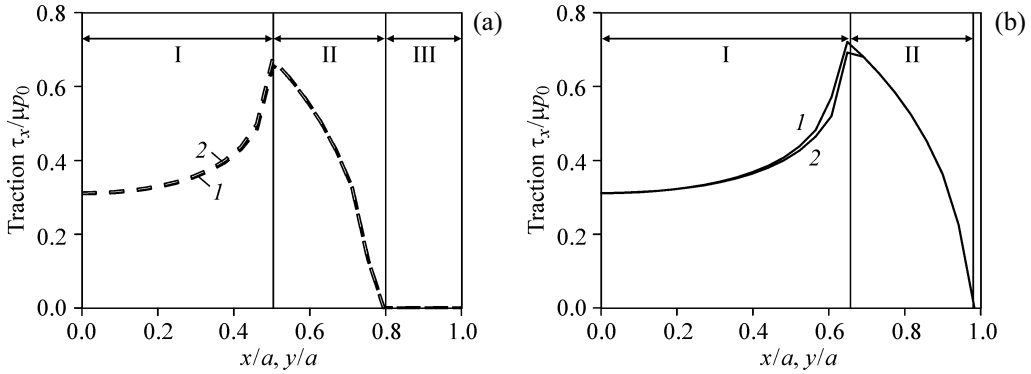

Fig. 5. Normalized tangential traction $\tau_x/\mu p_0$ along the center lines parallel (a) and perpendicular (b) to the direction of the rolling w for $w \| f_t$ (*1*) and $w \perp f_t$ (*2*) (3D-CONTACT model).

not be moved beyond the initial area of contact at any time. Thus, taken by itself, neither of the two factors leads to a failure of the contact.

3.1. Shakedown and Induced Microslip

The system response as a result to the oscillation is the same in both cases, parallel and perpendicular. Experiments and simulations show that the oscillatory rolling initially leads to an increase of the rigid body displacement with respect to the static value, as depicted in Fig. 4. We only report numerical results of the 3D CONTACT simulation here, see experimental results in [16].

The characteristic response can be explained as follows. At first, the system is in equilibrium due to the constant macroscopic forces, i.e. $u = u_{\text{stat}}$. The back- and forth movement of the sphere then alters the normal pressure distribution. It drops at the actual trailing edge and grows at the leading edge. Due to slipping and decreasing tangential stress at the trailing edge results an imbalance in the tangential direction. This increases the rigid body displacement and reduces the stick region within every rolling period.

In case that f_t and w fall below the shakedown limits, the displacement stops after a certain number of periods as depicted in Fig. 4a. The residual force within the contact is sufficiently strong to prevent any further slip and a shakedown occurs. Thus, the system reaches a new equilibrium and the displacement refers to the constant, time independent shakedown displacement $u = u_{\text{sd}}$ [13]. The entire contact region then remains in a state of stick, despite the fact that the rolling is continued.

Otherwise, if f_t and w exceed the shakedown limits, the contact fails and the displacement continues with the oscillation. This effect is referred to as frictional ratcheting or induced microslip. Here, one side of the contact alternately sticks, while the other slips, what leads to an accumulated displacement of the substrate, as depicted in Fig. 4b. Although both settings, $w \| f_t$ and $w \perp f_t$, show the same response, the magnitude of the shakedown displacement u_{sd} as well as the incremental displacement are higher for the perpendicular case if all other parameters are identical, as shown in Fig. 4.

3.2. Contact Region for the Shakedown Case

In the new equilibrium remain three characteristic contact regions. These are illustrated in Fig. 5, where the normalized tangential traction $\tau_x/\mu p_0$ for both cases is shown along the center lines aligned parallel (a) and perpendicular (b) with the particular rolling direction (dashed and solid center lines of Fig. 6). Here, p_0 depicts the maximum pressure at $x, y = 0$:

$$p_0 = \frac{2}{\pi} E^* \left(\frac{d}{R} \right)^{1/2}. \qquad (11)$$

In the center occurs a region of constant displacement, i.e. the stick zone (I). At the outside (III), the contact is periodically released due to the oscillation and the tangential traction vanishes $\tau_x = 0$. Additionally, region (II) occurs in which the tangential displacement is such, that the tangential stress equals μ times the minimum pressure, i.e. the traction bound which appears at the reversal points of oscillation. It shows that the region (III) almost vanishes for the perpendicular line (b).

In addition, the traction distribution slightly differs for both cases. Along the parallel center line (a), it is higher for the perpendicular setting. And vice versa, along the perpendicular center (b) line, it is higher for the parallel case. Regarding the normalized displacement of particles in contact $u_x(x, y)/U_0$ depicted in Fig. 6, it shows that the stick zone (I) is spindle shaped in both cases.

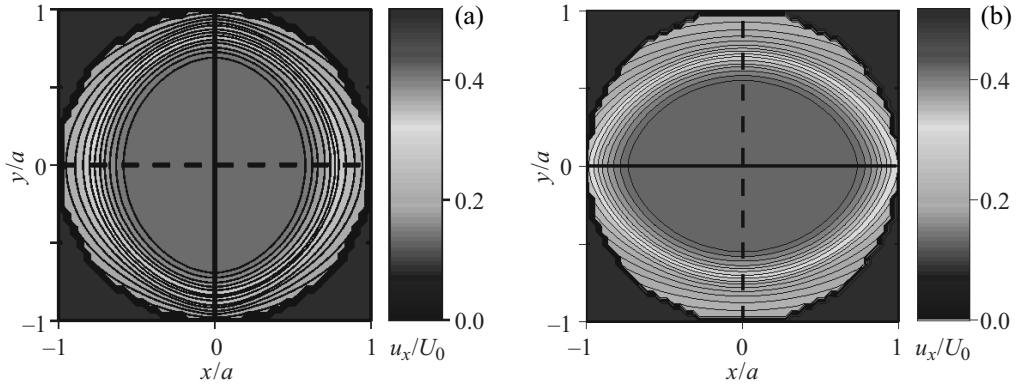

Fig. 6. Normalized tangential displacement u_x/U_0 after shakedown for $w \| f_t$ (a) and $w \perp f_t$ (b).

However, the displacement also slightly differs, as illustrated in Fig. 7, which shows u_x along the center lines. In accordance with the observations of Sect. 3.1, $u_x = u_{sd}$ in the stick zone (I) is higher for $w \perp f_t$. However, along the parallel center line in (II) and (III) u_x is higher for $w \| f_t$, as shown in Fig. 7a. The difference in the traction and displacement distribution is caused by the evolution of the contact in the course of the shakedown process. As a result, the direction of the oscillation influences the shakedown displacement u_{sd}.

4. RESULTS AND DISCUSSION

Using the model of the method of dimensionality reduction of Sect. 2.3 and the equilibrium condition of tangential forces, we get the following relation between loading, amplitude and displacement [15]:

$$f_t = 1 - \frac{3}{2} w u_{sd} - (1 - u_{sd})^{3/2}. \quad (12)$$

Due to the reasons mentioned in Sect. 2.3, this expression is initially the same for both cases. One assumption for the method of dimensionality reduction is rotational symmetry of the contact [23]. Consequently, a small deviation occurs in the relation between loading and oscillation amplitude (12), as the real contact region is spindle shaped in both cases. Considering this, a mapping parameter κ is introduced [16]:

$$f_t = 1 - \kappa w u_{sd} - (1 - u_{sd})^{3/2} \quad (13)$$

which is different for both cases, due to the influence of the rolling direction on the contact region. Comparison with the simulations and experiments yields the different mapping parameters of the two cases [16]:

$$\kappa_{\|} = 1, \kappa_{\perp} = 1.1. \quad (14)$$

Using Eq. (13) this gives:

$$w \| f_t \Rightarrow f_t = 1 - w u_{sd} - (1 - u_{sd})^{3/2}, \quad (15)$$

$$w \perp f_t \Rightarrow f_t = 1 - 1.1 w u_{sd} - (1 - u_{sd})^{3/2}. \quad (16)$$

Figure 8 shows the shakedown displacement as a function of f_t for different w.

Dotted lines are computed with Eq. (15) and solid lines are computed with Eq. (16). The error bars and marks show experimental results for $w \perp f$ (see experiments for $w \| f$ in [16]). The asterisks indicate simulations for $w \perp f$, where values close to the shakedown limit are not given because CONTACT lacks accuracy close to the traction bound [22]. Comparison of the theo-

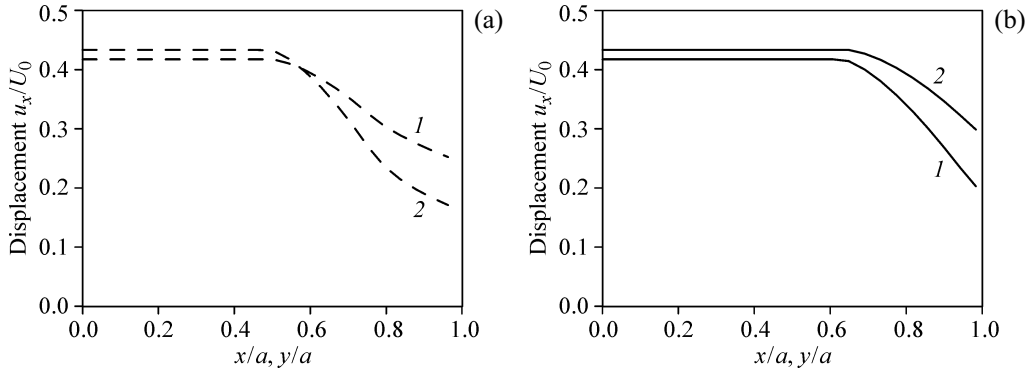

Fig. 7. Normalized tangential displacement u_x/U_0 along the center lines parallel (a) and perpendicular (b) to the direction of the rolling w for $w \| f_t$ (*1*) and $w \perp f_t$ (*2*) (3D-CONTACT model).

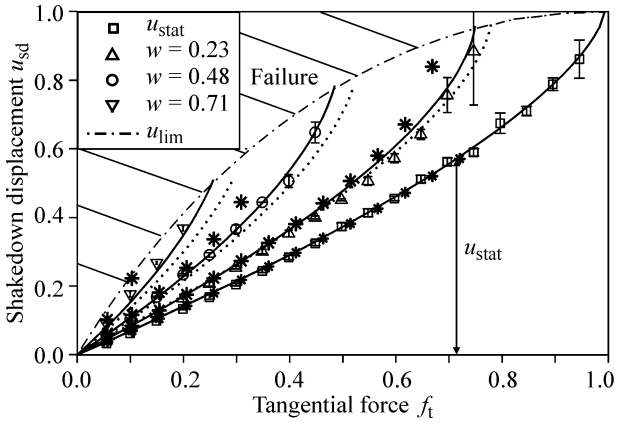

Fig. 8. Shakedown displacement of the substrate u_{sd} as a function of the tangential force f_t for different oscillation amplitudes w. The oscillatory rolling causes an increase of the displacement by comparison with its static value u_{stat}. Analytical (solid lines), experimental (error bars and marks) and three-dimensional simulation (asterisks) results.

retical, experimental and numerical results shows that the shakedown displacement u_{sd} is higher for a perpendicular setting than for a parallel one. It must be noted that in case that the oscillation stops to soon, the final displacement might differ from this theoretical shakedown value [13]. In the experiments, the shakedown state was reached after $n \approx 10$ periods. The dashed line gives the maximum displacement for a given amplitude, that is reached before complete sliding occurs and the contact fails:

$$u_{lim} = 1 - w_{lim}^2. \tag{17}$$

Although this expression is the same for both cases, the relations between maximum tangential load and amplitude differ slightly. These can be derived using the condition that the stick region vanishes in the maximum [16]

$$w \| f_t \Rightarrow f_{t,lim} = 1 - w_{lim}, \tag{18}$$

$$w \perp f_t \Rightarrow f_{t,lim} = 1 - 1.1 w_{lim} + 0.1 w_{lim}^3. \tag{19}$$

Experimentally, the maxima were identified by a stepwise increase of the amplitude, while the tangential force was kept constant. Thus, figure 9 shows w_{lim} as a function of $f_{t,lim}$. Again, experimental results are illustrated with marks and error bars and are only given for $w \perp f$. The theoretical values are represented by the dotted (Eq. (18)) and solid lines (Eq. (19)). It shows that w_{lim} is slightly lower for $w \perp f$. However, the difference is in the range of the relative deviation. Additionally, figure 10 shows the maximum shakedown displacement illustrated with asterisks and the displacement in case of induced microslip after five oscillation periods marked by triangles.

Equations (18) and (19) correspond to the exact analytical shakedown cases for $w \| f$ and $w \perp f$. For a given amplitude, one can thus compute the maximum tangential force to achieve a safe shakedown and vice versa. The results show that shakedown is accompanied with a significant reduction of the loading capacity as $f_{t,lim} \le 1$ in both cases. Additionally, for the same amplitude, the parallel setting could theoretically bear slightly higher tangential load, but the difference is only minor. Thus, in force-locked joints with oscillations of this type, it might be more convenient if tangential loading and oscillation are aligned parallel.

If the shakedown limits are exceeded, the contact fails and induced microslip occurs. In dependence on the actual rolling direction, one side of the contact sticks, while the other slips. This accumulated displacement results in an rigid body motion referred to as walking [6]. As shown in Fig. 11, the incremental displacement Δu increases with f_t and w.

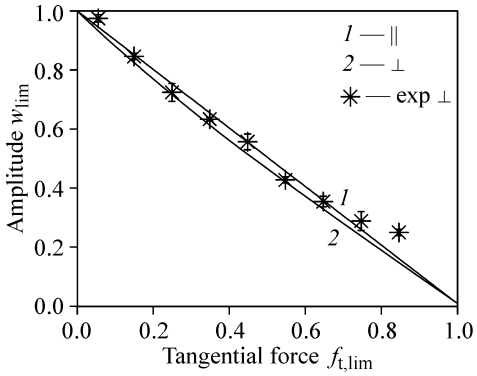

Fig. 9. Maximum amplitude w_{lim} as a function of the tangential force $f_{t,lim}$ for $w \perp f_t$. Asterisks show experimental results, solid lines give the theoretical value.

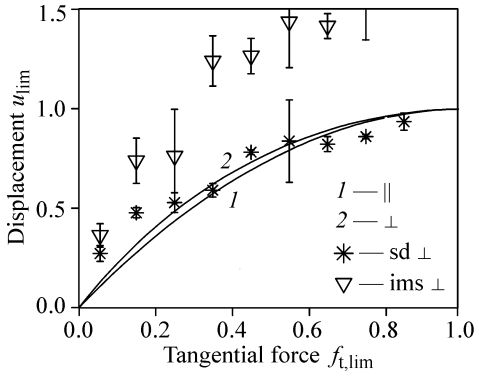

Fig. 10. Maximum displacement u_{lim} as a function of the tangential force $f_{t,lim}$ for $w \perp f_t$. Shakedown displacement (asterisks) and induced microslip displacement after five periods (triangles).

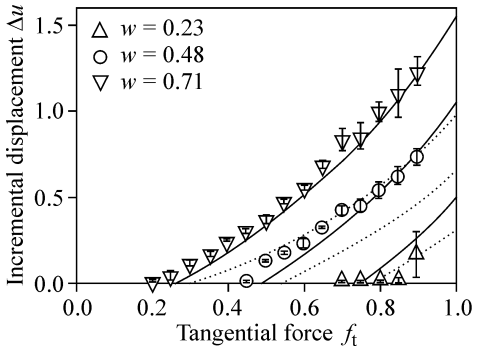

Fig. 11. Incremental displacement Δu as a function of the tangential force f_t for different amplitudes w for $w \perp f_t$. Solid lines depict theoretical values and error bars and marks denote experimental results.

Here the experimental results for $w \perp f_t$ are illustrated by marks and error bars. The dotted $(w \| f_t)$ and solid $(w \perp f_t)$ lines show the approximation functions which are derived using a linear regression procedure with u_{stat} as the regressor [15]. The incremental displacements differs for both cases:

$$w \| f_t \Rightarrow \Delta u \approx \sqrt{2(1-(1-f_t)^{2/3})}(w - w_{lim}), \quad (20)$$

$$w \perp f_t \Rightarrow \Delta u \approx \sqrt{5(1-(1-f_t)^{2/3})}(w - w_{lim}). \quad (21)$$

It is significantly higher for the perpendicular setting. This microslip effect can be used for the generation of small displacement in case that an increase of the tangential loading is not possible or high accuracy is needed as in MEMS devices. In both cases, the perpendicular setting is more convenient as it generates a higher displacement.

5. CONCLUSION

We examined a quasi-static frictional system of a rigid sphere and an elastic substrate. Coulomb friction with constant μ and a steady macroscopic load regime was assumed. In addition the system was from an uncoupled type, meaning that a varying normal force will not induce a displacement in the tangential direction and vice versa.

We considered slight oscillatory rolling of the sphere in different directions, namely parallel and perpendicular to the tangential load. In both cases, the rolling alters the normal pressure distribution and the contact region, what leads to partial slip and a macroscopic rigid body displacement. If the oscillation amplitude and the tangential force fall below the shakedown limits, the displacement stops and shakedown occurs. Otherwise, the contact fails and the displacement continues as a consequence of the ratcheting effect.

We derived the analytical shakedown limits for both cases, parallel and perpendicular, and showed that shakedown is accompanied with a significant decrease of the tangential load capacity. In addition, we can predict the rigid body displacement in case of shakedown and the incremental displacement in case of ratcheting. It was shown that the rolling direction leads to differences in the contact region and the tangential traction. As a consequence, both the shakedown displacement and the incremental displacement are higher for the perpendicular setting. Future research is needed, to examine arbitrary settings with angles between 0° and 90°. Additionally, the interaction of oscillating forces and the rolling should be considered. It is also important to examine different contact geometries, especially for technical applications.

REFERENCES

1. Chung, K. and Ip, K., Finite Element Modeling of Bolted Connections between Cold Formed Steel Strips and Hot Rolled Steel Plates under Static Shear Loading, *Eng. Struct*., 2000, vol. 22, pp. 1271–1284.
2. Li, B., Melkote, S.N., and Liang, S.Y., Analysis of Reactions and Minimum Clamping Force for Machining Fixtures with Large Contact Areas, *Int. J. Adv. Manuf. Tech*., 2000, vol. 16, pp. 79–84.
3. Booker, J.D., Truman, C.E., Wittig, S., and Mohammed, Z., A Comparison of Shrink-Fit Holding Torque Using Probabilistic, Micromechanical and Experimental Approaches, *Proc. Inst. Mech. Eng. B: J. Eng. Manuf*., 2004, vol. 218, pp. 175–187.
4. McCarthy, C.T., McCarthy, M.A., Stanley, W.F., and Lawlor, V.P., Experiences with Modeling Friction in Composite Bolted Joints, *J. Compos. Mater*., 2005, vol. 39, pp. 1881–1908.
5. Law, S.S., Wu, Z.M., and Chan, S.L., Analytical Model of a Slotted Bolted Connection Element and its Behavior under Dynamic Load, *J. Sound Vib*., 2006, vol. 292, pp. 777–787.
6. Mugadu, A., Sackfield, A., and Hills, D.A., Analysis of a Rocking and Walking Punch. Part I: Initial Transient and Steady State, *J. Appl. Mech*., 2004, vol. 71, pp. 225–233.
7. Hartwigsen, C.J., Song, Y., McFarland, D.M., Bergman, L.A., and Vakakis, A.F., Experimental Study of Non-Linear Effects in a Typical Shear Lap Joint Configuration, *J. Sound Vib*., 2004, vol. 277, pp. 327–351.
8. Huq, M.Z. and Celis, J., Fretting Fatigue in Alumina Tested under Oscillating Normal Load, *J. Am. Ceramic Soc*., 2002, vol. 85, pp. 986–988.
9. Nowell, D., Dini, D., and Hills, D., Recent Developments in the Understanding of Fretting Fatigue, *Eng. Fract. Mech*., 2006, vol. 73, pp. 207–222.

10. Antoni, N., Nguyen, Q.-S., Ligier, J.-L., Saffré, P., and Pastor, J., On the Cumulative Microslip Phenomenon, *Eur. J. Mech. A. Solids*, 2007, vol. 26, pp. 626–646.
11. Churchman, C.M. and Hills, D.A., General Results for Complete Contacts Subject to Oscillatory Shear, *J. Mech. Phys. Solids*, 2006, vol. 54, pp. 1186–1205.
12. Melan, E., Theorie statisch unbestimmter Systeme aus ideal-plastischem Baustoff, *S.-B. Akad. Wiss. Wien. Math.-nat. Kl. II a*, 1936, vol. 145, pp. 195–218.
13. Klarbring, A., Ciavarella, M., and Barber, J.R., Shakedown in Elastic Contact Problems with Coulomb Friction, *Int. J. Solids Struct*., 2007, vol. 44, pp. 8355–8365.
14. Barber, J.R., Klarbring, A., and Ciavarella, M., Shakedown in Frictional Contact Problems for the Continuum, *Comptes Rendus Mécanique*, 2008, vol. 336, pp. 34–41.
15. Wetter, R., Shakedown and Induced Microslip of an Oscillating Frictional Contact, *Phys. Mesomech*., 2012, vol. 15, no. 5–6, pp. 293–299.
16. Wetter, R. and Popov, V.L., Shakedown Limits for an Oscillating, Elastic Rolling Contact with Coulomb Friction, *Int. J. Solids Struct*., 2014, vol. 51, no. 5, pp. 930–935.
17. Ahn, Y.J., *Response of Coupled Frictional Contacts to Cyclic Loading*, Ann Arbor: UMI Dissertation Publ., 2011.
18. Popov, V.L., *Contact Mechanics and Friction: Physical Principles and Applications*, Berlin: Springer-Verlag, 2010.
19. Ciavarella, M., Tangential Loading of General Three-Dimensional Contacts, *J. Appl. Mech*., 1998, vol. 65, pp. 998–1003.
20. Jäger, J., A New Principle in Contact Mechanics, *J. Tribology*, 1998, vol. 120, pp. 677–684.
21. Kalker, J.J., *Three-dimensional Elastic Bodies in Rolling Contact. Solid Mechanics and its Applications*, Dordrecht: Kluwer Academic Publishers, 1990.
22. Vollebregt, E.A.H., User Guide for Contact, Vollebregt and Kalker's Rolling and Sliding Contact Model, Vortech Computing, Delft, http://www.kalkersoftware.org/downloads/user-guide.pdf. Accessed November 11, 2013.
23. Heß, M., *Über die exakte Abbildung ausgewählter dreidimensionaler Kontakte auf Systeme mit niedrigerer räumlicher Dimension*, Göttingen: Cuvillier-Verlag, 2011.
24. Popov, V.L. and Heß, M., *Methode der Dimensionsreduktion in Kontaktmechanik und Reibung, Eine Berechnungsmethode im Mikro- und Makrobereich*, Berlin: Springer-Verlag, 2013.
25. Popov, V.L. and Psakhie, S.G., Numerical Simulation Methods in Tribology, *Tribol. Int*., 2007, vol. 40, pp. 916–923.
26. Popov, V.L., Method of Reduction of Dimensionality in Contact and Friction Mechanics: A Linkage between Micro and Macro Scales, *Friction*, 2013, vol. 1, no. 1, pp. 41–62.